International Journal of Advanced Engineering Research and Science (IJAERS)
Peer-Reviewed Journal
ISSN: 2349-6495(P) | 2456-1908(O)
Vol-9, Issue-3; Mar, 2022
Journal Home Page Available: https://ijaers.com/
Article DOI: https://dx.doi.org/10.22161/ijaers.93.35

Improved Hydrodynamic Efficiency of Kaplan Hydro Turbine through Varying Blade Number and Length

Olusegun Balogun[1], Victoria Alao[2], Babatope Pele[3], L.L Ladokun[4]

[1]Federal University of Agriculture Abeokuta
[2]University of Ilorin
[3]University of Ibadan
[4]National Centre for Hydropower Research and Development, University of Ilorin
Corresponding Author email: peleolabanji@gmail.com

Received: 10 Jan 2022,

Received in revised form: 10 Mar 2022,

Accepted: 20 Mar 2022,

Available online: 31 Mar 2022

Keywords *—* ***Kaplan hydro turbine, CFD, Hydrodynamics, Renewable energy, Blade number.***

Abstract *— Kaplan hydro turbines are adjustable propeller blade turbines that are used in conventional hydroelectric power systems for the generation of electric power. Their mechanical efficiency based on their flexible and wide operating range of flow rates and head depends much on the runner blades and the alignments of the wicket gates. However, design modification of the geometry of the runner blade can be made for the improvement of mechanical efficiency. Computational Fluid dynamics simulation was employed to investigate the improved features of two hypothetical model turbine blades. SolidWorks® software was used for modeling the two categories of the turbine, named model A and model B Kaplan turbines. Model A has a short blade length of 130 mm twisted at an angle of 300, and its blade was varied from 2 to 6 blades. Model B has a longer blade length of 150 mm twisted at an angle of 300, and its blade was varied from 2 to 6 blades. The governing equations, which include continuity and momentum, were discretized using the Finite Volume method. The result shows that an increase in blade total surface area, as a result of an increase in blade length or blade number, increases the power output of the Kaplan hydro turbine.*

INTRODUCTION

Hydropower which is an important renewable energy resources refers to the energy generated when water is used in turning rotor-dynamic machineries to generate electric power. This can be achieved through the conventional dam hydro-electric facilities or through the currents in oceans, tidal, rivers, and artificial water channels in form of hydrokinetic technologies (Chica et al., 2016) Hydro-to-electric power system, which is being strongly recognized as a unique renewable energy solution (Khan et al., 2007) and producing electricity by using hydropower plant is most suitable in rural areas, as it is effective and cheap (Elbatran et al, 2015). The hydropower turbines consist of many functional components, but one of the most important functional components responsible for the overall power supply is known as the “turbine rotor”. In general, a rotor consists of blades connected to a central hub that ultimately provides the shaft to transmit torque to the system. The blade design needs to be carefully considered due to the effect of its power coefficient (Chica et al., 2018).

Hydraulic Turbines are rotary machines that convert kinetic energy or potential energy of water into mechanical work. There are two typically major types of hydropower turbine which are Impulse and Reaction turbines. Reaction turbines rely on a pressure drop in the water across the turbine to transfer energy to the shaft while impulse turbines transfer the moment of a high velocity water jet to

the turbine (Thake, 2000). Examples of Reaction turbines are Kaplan and Francis turbine while Impulse turbines are Turgo, Pelton and Cross-flow turbines. The works of Cengel and Cimbala (2006) and OEERE (2021) also confirmed these types of hydro turbines as shown below:

Table 1.0 Classification of the turbines base on its head, flow rate and specific speed; Source: (Jawad, 2019)

Type	Head	Flow rate	Specific Speed
Pelton Turbine	High	Low	Low
Francis Turbine	Medium	Medium	Medium
Kaplan Turbine	Low	High	High

Reaction turbines often have complex blade geometries and housings, which make them more difficult to manufacture at smaller scales in a developing country setting. Kaplan turbine is a propeller-type water turbine which has adjustable blades. It has been considered one of the best hydro turbines due to its operation for high flow rate and low head. Kaplan is an evolution of Francis turbine which allows efficient power production at any available low head. Its low head ranges from 10-70 meters while its runner diameter usually ranges from 2-11metres.The inward fluid flow for reaction turbine e.g. Kaplan turbine involves changing pressure of its working fluid as it flows through the turbine to generate its energy. Power is gotten from its hydrostatic head and kinetic energy of the flowing fluid. Therefore, Kaplan turbine comprises of both design features from radial and an axial turbine. Generally, the hydropower schemes are classified to cover a broad range of power output as below.

Table 2.0: Classification and power output (Jawad, 2019)

Classification	Power Output
Large	>100MW
Small	10-100MW
Medium	1-10MW
Mini	100KW-1MW
Micro	5-100KW
Pico	<5KW

Various studies have been done to improve its hydrodynamic efficiency through the modification of the geometry of some component parts. From the study of Dixon, (2005), optimization of the runner blade design brought about improved power generation through the extraction of more water energy. CFD simulations was done to study the flow on the blade of a hydro turbine, the results showed the efficiency was affected by pressure distribution on the turbine runner blade (Nuantong, 2009). Bashir et al., (2012) also investigated the experimental and CFD simulation predicted power outputs of a Kaplan turbine. Both results were quite similar; where CFD results showed slightly lesser values to the experimental values in most of the flow rates.

Chamil et al., (2017) studied the design of a Kaplan turbine runner wheel. Theoretical design was initially performed for determining the main characteristics where it showed an efficiency result of 94%. Usually, theoretical equations are generalized and simplified and also, they assume constants of experienced data and hence a theoretical design will only be an approximate. This was confirmed as the same theoretical design showed only 59.98% of efficiency with a computational fluids dynamics (CFD) evaluation. Finally, an optimization design was further analyzed where pressure distribution and inlet/outlet tangential velocities of the blades were analyzed and corrected with CFD to improve the efficiency of power generation. The original design could be improved to achieve an efficiency of 93.01%. The blades' inlet/outlet angles also showed a significant influence on the turbine's power output.

From Sotoude et al., (2019), development of design method numerically was presented for axial hydraulic turbine with very low head and validated with experimental data. The results show that the hydraulic efficiency was affected by rotational turbine speed and runner blade angle. Andrej et al, (2019) used computer aided flow visualization to investigate the cavitation phenomena on the Kaplan runner blade for a modified turbine. Results showed that cavitation phenomena were reduced, power output and performance were increased for the modified Kaplan turbine. The design of a micro hydraulic turbine was made to work in a small amount of power to provide energy for a number of houses.

Numerical investigation characteristics of flow through low head Kaplan turbine runner was carried out to predict and improve the overall performance of a mini hydro turbine (Jawad, 2019). The performance of a micro Kaplan turbine was been predicted such as power output and efficiency. Furthermore, the effect of blades number showed a significant influence on the turbine's power output and efficiency.

CFD Simulation using ANSYS Workbench 16

The theoretically proposed Kaplan turbine designs were modeled using the software ANSYS Design Modeler. In

ANSYS Design Modeler, the turbine blades for both models were imported and enclosed with a rectangular shroud. The blade rotation region was also cylindrical enclosed for the purpose of flow simulation to achieve an optimum performance of Kaplan Turbine. The head (H) of 6m and a constant velocity of water flow V of 20ms-1 are considered for both blade models. The preliminary design of the shroud was based on the net available head at inlet and the discharge in the turbine system. The surface areas for 2 to 6-blade runners in model A are 0.027m2, 0.038m2, 0.048m2, 0.057m2 and 0.062m2 respectively. The surface areas for the 2-blade runner to 6-blade runner in model B are 0.035m2, 0.049m2, 0.062m2, 0.075m2 and 0.084m2 respectively. The more the number of blades on the runner, the higher the surface area.

Table 3.0 Input parameters of Kaplan turbine blade for model A and B

Parameter	Symbol	Value
Net Head	H_N	4m
Suction Head	H_S	2m
Gross Head	H	6m
Hub diameter	D_i	0.003m
Runner diameter	D_e	0.1m
Inlet Flow velocity of water	w_m	20m/s

In this study, the Navier–Stokes and continuity equations have been used in the x, y and z directions to describe the flow. The governing equations can be expressed as (Bose, 1997):

Continuity: $\frac{\partial(\rho u)}{\partial x} + \frac{\partial(\rho v)}{\partial y} + \frac{\partial(\rho w)}{\partial z} = 0$ 1

X-Momentum: $\frac{\partial(\rho u)}{\partial t} + u\frac{\partial(\rho u)}{\partial x} + v\frac{\partial(\rho u)}{\partial y} + w\frac{\partial(\rho u)}{\partial z} = \left(-\frac{\partial p}{\partial x} + \mu_f\left[\frac{\partial^2 u}{\partial x^2} + \frac{\partial^2 u}{\partial y^2} + \frac{\partial^2 u}{\partial z^2}\right]\right)$ 2

Y-Momentum: $\frac{\partial(\rho v)}{\partial t} + u\frac{\partial(\rho v)}{\partial x} + v\frac{\partial(\rho v)}{\partial y} + w\frac{\partial(\rho v)}{\partial z} = \left(-\frac{\partial p}{\partial y} + \mu_f\left[\frac{\partial^2 v}{\partial x^2} + \frac{\partial^2 v}{\partial y^2} + \frac{\partial^2 v}{\partial z^2}\right]\right)$ 3

Z-Momentum: $\frac{\partial(\rho w)}{\partial t} + u\frac{\partial(\rho w)}{\partial x} + v\frac{\partial(\rho w)}{\partial y} + w\frac{\partial(\rho w)}{\partial z} = \left(-\frac{\partial p}{\partial z} + \mu_f\left[\frac{\partial^2 w}{\partial x^2} + \frac{\partial^2 w}{\partial y^2} + \frac{\partial^2 w}{\partial z^2}\right]\right)$ 4

Velocity Triangle of Kaplan Turbine Blade

In order to know the blade angle of each section, velocity diagram is drawn for each section. Different velocities such as tangential velocity, flow velocity, and whirl velocity are shown in the figure. Gratings, as mentioned in the figure, occur by a cylindrical cut (developed into drawing pane) at the runner. The first velocity triangle occurs when the water just enters into the runner (before the grating), and the other velocity triangle occurs at the time when water leaves the runner (after the grating). The vertical components wm_1 and wm_2 are flow velocities and are equal. The relative velocity w_∞ can be determined by taking an average of relative velocity at the inlet (w_1), and relative velocity at the outlet (w_2) and β_∞ shows its direction.

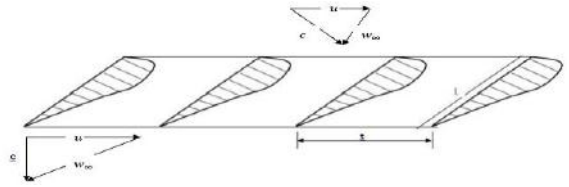

Fig.2.0: Schematic of blades' cross sections and velocity triangles (Chamil and Tobi, 2017)

Where,

w_∞ = Relative Velocity magnitude[m/s]

c = Velocity Magnitude [m/s]

u = Tangential Velocity [m/s]

Drawing velocity triangle at each section of the blade and using following equations, tangential velocity, inlet velocity, radial velocity, velocity magnitude, relative velocity magnitude and blade angle at each section are calculated (Chamil and Tobi, 2017).

Tangential velocity (u); $u = \pi * d * n$ 5

Velocity magnitude (C_u); $C_u = \frac{H_n * g}{u}$ 6

Vorticity magnitude (w_u); $w_u = C_u - u$ 7

Flow Velocity or inlet velocity (w_m);

$w_m = \frac{Q}{A} = \frac{Q}{\frac{\pi}{4} * (D_e{}^2 - D_i{}^2)}$ 8

Relative Velocity magnitude (w_∞) $w_\infty = \sqrt{w_u^2 + w_m^2}$ 9

Blade Angle (β_∞),

$\beta_\infty = 90 - tan^{-1}\frac{w_u}{w_m}$ 10

Axial force (F_a); $F_a = \rho * g * H_n * A_b$ 11

where, A_b is the area of the blade $= \frac{\pi * \alpha * (R_e^2 - R_i^2)}{360}$ 12

where α is tilting angle of turbine blade at 30°

Discretizing Governing Flow Equations using Finite Volume Method (FVM)

The numerical algorithm step for finite volume method involved the governing equations for incompressible two dimensional such as continuity equation and Navier Stroke Equation was set. The Second step in the finite volume method was to divide the domain into discrete control volumes. Nodal points were placed in the space of the flow rectangular geometry. The boundaries (or faces) of control volumes were positioned mid-way between adjacent nodes. Thus, each node is surrounded by a control volume or cell. Discretization using Formal integration of the governing equations of fluid flow over all the control volumes of the solution domain representing flow process such as convection, diffusion and sources. The integral equations were converted to a system of algebraic equation. An iterative method was used to solve the algebraic equations and results were presented graphically.

Turbulence Realizable k-ε Model

K-epsilon (k-ε) turbulence model is the most common model used in computational fluid dynamics (CFD) to simulate mean flow characteristics for turbulent flow conditions. It is a two-equation model which gives a general description of turbulence by means of two transport equations; the turbulent kinetic energy k and the turbulence eddy dissipation ε (i.e., the rate at which the turbulent kinetic energy dissipates).

The transport equations in this model are written as:

$$\frac{\partial k}{\partial t} + \frac{\partial k u_i}{\partial x_i} = \frac{\partial}{\partial x_i}\left(D k_{eff} \frac{\partial k}{\partial x_i}\right) + G_k - \varepsilon \quad (13)$$

$$\frac{\partial \varepsilon}{\partial t} + \frac{\partial \varepsilon u_i}{\partial x_i} = \frac{\partial}{\partial x_i}\left(D \varepsilon_{eff} \frac{\partial \varepsilon}{\partial x_i}\right) + \sqrt{2} c_{1\varepsilon} S_{ij} \varepsilon - C_{2\varepsilon} \frac{\varepsilon^2}{k + \sqrt{v\varepsilon}} \quad (14)$$

Where C_μ is computed by:

$$v_f = C_\mu \frac{k^2}{\varepsilon} \quad (15)$$

$$C_\mu = \frac{1}{A_0 + A_s \frac{k u^*}{\varepsilon}} \quad (16)$$

$$u^* = \sqrt{s_{ij} s_{ij} + \widetilde{\Omega_{ij}} \widetilde{\Omega_{ij}}} \quad (17)$$

$$\widetilde{\Omega_{ij}} = \widetilde{\Omega_{ij}} - \varepsilon_{ijk} \omega_k \quad (18)$$

Where $\widetilde{\Omega_{ij}}$ is the mean rate of rotation tensor and ω_k is the angular velocity. The constants A_0 and A_s are determined as below:

$$A_0 = 4, A_s = \sqrt{6} cos\varphi$$

$$\varphi = \frac{1}{3} Arc \cos\left(min\left(max\left(\sqrt{6}W, -1\right), 1\right)\right) \quad (19)$$

$$W = \frac{s_{ij} s_{jk} s_{ki}}{\widetilde{S^2}} \quad (20)$$

$$c_{1\varepsilon} = max\left(\frac{\eta}{5+\eta}, 0.43\right) \quad (21)$$

$$\eta = S\left(\frac{k}{\varepsilon}\right) \quad (22)$$

Fluid Flow Velocity around Different Blades of the Model A Kaplan Turbine

The velocity contours of the runner blades of the model A Kaplan turbine generated by the fluid energy are represented in figure 3.0. The figure showed the fluid flow in z-axis and y-axis, moving against the runner blade and the lateral velocity profile as well as the quality of the wake developed. The results showed the maximum velocity obtained was for the 2-blade runner, which was 126.44ms-^{1}, for the 3-blade runner, the value obtained was 145.29ms-^{1}, for 4-blade runner was 125.375ms-^{1}, for 5-blade runner was 137.721ms-^{1}, for 6-blade runner was 131.881ms-^{1}.

The 3-blade runner also showed the highest velocity, followed by 5-blade runner while 4-blade runner showed the lowest value of velocity followed by the 2-blade runner. However, for model A, irrespective of the blade numbers, maximum velocity was observed at the tip of the runner blade while minimum velocity occurs at the blade hub. Table 4.0 presents the different blades, their areas and fluid flow velocities around them.

Table 4.0: Blade surface area and its flow rate

Number of Blades	Blade surface area model A (m^2)	Blade surface area model B (m^2)	Increase in surface area between Model A and B (m^2)	Flow Rate around runner blade model A(m^3/s)	Flow Rate around runner blade model B(m^3/s)
2 Blades	0.027	0.035	0.008	0.541	0.699
3 Blades	0.038	0.049	0.011	0.760	0.980
4 Blades	0.048	0.062	0.014	0.960	1.245
5 Blades	0.057	0.075	0.018	1.134	1.497
6 Blades	0.062	0.084	0.022	1.242	1.682

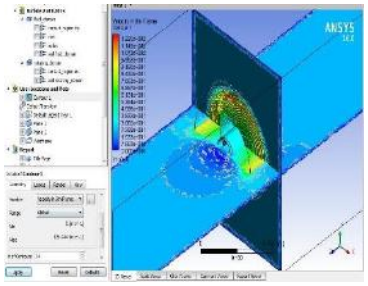

(a) 2-blades runner

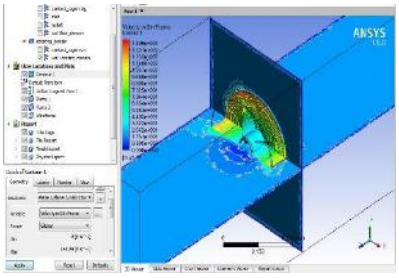

(b) 3-blades runner

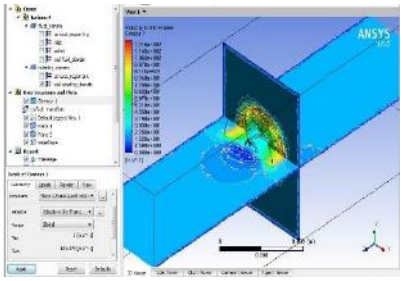

c) 4-blades runner

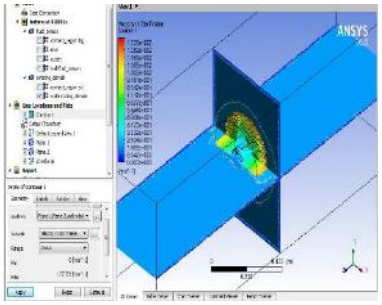

(d) 5-blades runner

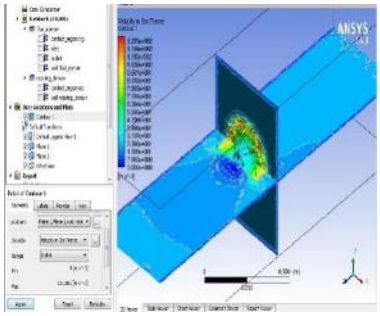

(e) 6-blades runner

Fig.3.0 Velocity for 2 to 6-Blade Runner of Model a Kaplan Turbine

Fluid Flow Velocity around Different Blades of the Model B Kaplan Turbine

The velocity contours of the runner blades of the model A Kaplan turbine generated by the fluid energy are represented in figure 4.0. Model B design was based on an increase in total surface area to that of model A. The surface areas for the two-bladed runner to six-bladed runner in model B are $0.035m^2$, $0.049m^2$, $0.063m^2$, $0.075m^2$ and $0.084m^2$ respectively. The figure 4.0 showed the fluid flow in z-axis and y-axis, moving against the runner blade and the lateral velocity profile as well as the quality of the wake developed. The results showed the maximum velocity obtained was for the two-bladed runner, which was $144.667ms^{-1}$, for 3-blade runner was $206.94\ ms^{-1}$, for 4-blade runner was $153.54ms^{-1}$, for 5-blade runner was $174.802ms^{-1}$, for 6-blade runner was $159.371ms^{-1}$.

The 3-blade runner also showed the highest velocity, followed by 5-blade runner while 4-blade runner showed the lowest value of velocity followed by the 2-blade runner. However, for respective blade number for model B maximum velocity was observed at the tip of the runner blade while minimum velocity occurs at the blade hub. The water vortices generation was observed on the water surface due to friction between the blade surface and the fluid. Three blades runner having the highest velocity was observed to have the highest formation of vortices on the surface of the fluid at both z-axis and y-axis. 2-blade runners having the lowest velocity were observed from figure 4.0 to have the smallest formation of vortices on fluid surface along z-axis and y-axis.

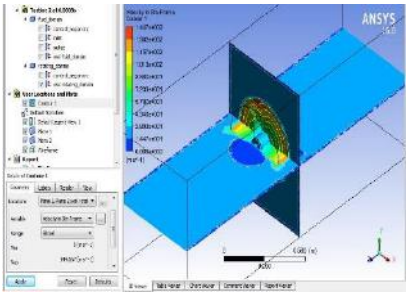

(a) 2-blades runner

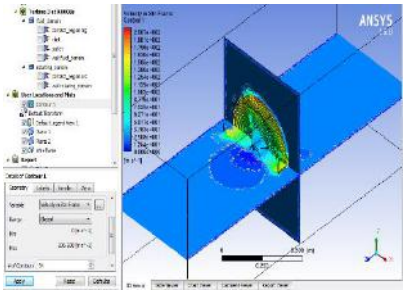

(b) 3-blades runner

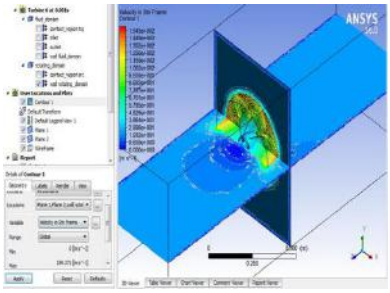

c) 4-blades runner

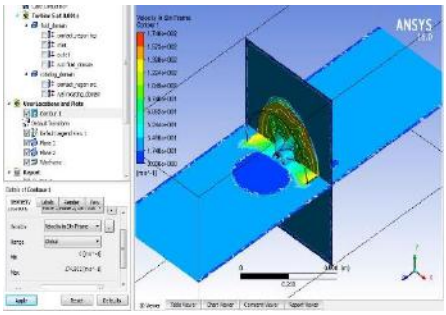

(d) 5-blades runner

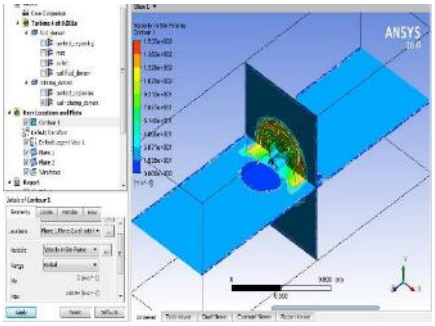

(e) 6-blades runner

Fig.4.0: Velocity for 2 to 6-Blade Runner of Model B Kaplan Turbine

Table 5.0: 2 to 6 runner blade velocities for model A and model B Kaplan Turbine

Number of Blades	Runner blade Model A velocity (m/s)	Runner blade Model B velocity (m/s)
2 Blades	126.444	144.667
3 Blades	145.29	206.938
4 Blades	125.375	153.54
5 Blades	137.721	174.802
6 Blades	131.881	159.371

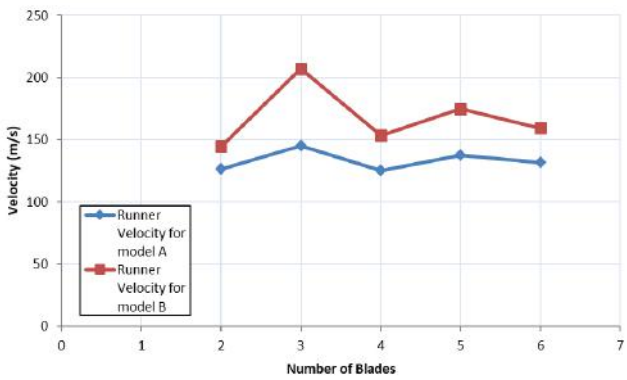

Fig. 5.0: Effect of blade numbers on Velocity

Effect of Blade Number on Velocity of Turbine Runner

The velocities from ANSYS 16 simulation is the velocity obtained from moving fluid required to rotate turbine blades domain. These results were gotten from ANSYS simulation results showing the reaction of water flow on the turbine blades varied from 2-blades to 6-blades at two different models. The flow ratio obtained is 9.68. Model A has a small blade surface area compared to model B which has a large surface area with the same twist angle of 300 at respective blade number of 2 to 6-blade runners. The simulation result contours shown above (Figures 3.0 and 4.0) were all set into two different planes, which are plane XY, plane XZ.

Figure 3.0 for model A and figure 4.0 for model B showed post simulation result for respective blade runner velocity which was extracted into table 4.1 above. It is observed from Figure 3.0, in Model A that the highest velocity obtained is with the 3-blade runner turbines which has a velocity value of 145.29m/s. From blade four to six, it was observed the more the addition of blades, the lower the velocity value. For Model B, 3-blade turbine runner also had the highest velocity value of 206.94m/s. After the 3-blade runner for model A and B, 5-blade runner shows the next highest turbine velocity for both model designs. Hence, it can be inferred, as already established from literature, that a low velocity had an adverse effect on the shaft rotation and hence power output of a turbine.

From Figure 5.0, all model B blade classifications show a higher value in velocity when compared with model A. Therefore, model B with 3 blades was observed as the best Kaplan blade design above Model A. This also shows that an increase blade surface area of a Kaplan turbine increases the velocity of runner blade thus improving the efficiency of the turbine. From Figure 6.0, it can also be observed that model B which has an

increased blade length gave higher velocity than model A. This shows the more the length of the blade, the better the velocity.

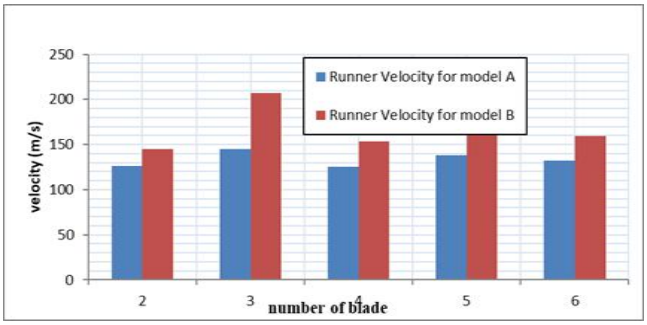

Fig.6.0: Chart presenting Model B with Increased Length showing Higher Velocity Magnitude than Model A.

Various Velocities profile for turbine blades

Various velocities considered for Kaplan blade design efficiency are axial velocity, velocity magnitude, radial velocity, tangential velocity, relative velocity magnitude, relative tangential velocity and vorticity magnitude which are shown in table 5.0. The result was generated from ANSYS 16.0-time simulation of 200 runs. Relative velocity magnitude is the velocity in relative to the rectangular turbine shroud. The analysis of result is shown in figure 6.0. Result shows the turbine having three blades for both model A and model B has the highest relative velocity magnitude above every other number of blades. Turbine having five blades has the second highest relative velocity magnitude for both model A and model B. However, Model B relative velocity magnitude value is higher than design Model A for all turbine number of blades from table 5.0. The vorticity magnitude shows the level of recirculation occurrence during fluid flow on the turbine blades

Table 6.0: Turbine Blade Velocities Profile obtained from ANSYS 16.0

	Parameter	**Unit**	**Blade 2**	**Blade 3**	**Blade 4**	**Blade 5**	**Blade 6**
Model A	Velocity-magnitude	m/s	21.92	22.76	22.92	23.05	22.81
Model B			22.24	23.19	23.11	23.41	23.37
Model A	Axial	m/s	19.62	19.60	19.59	19.59	19.53
Model B			19.67	19.67	19.68	19.64	19.63
Model A	Radial	m/s	0.30	0.51	0.43	0.37	0.48
Model B			0.22	0.29	0.41	0.41	0.49
Model A	Tangential	m/s	2.84	3.90	4.28	4.40	3.84
Model B			3.03	3.96	3.89	4.26	4.16
Model A	Relative-Velocity-Magnitude	m/s	160.62	168.81	158.45	161.97	159.19
			185.94	197.65	183.80	190.27	183.55
Model A	Vorticity magnitude	1/s	184.86	189.17	232.63	210.84	239.95
Model B			163.28	162.75	216.15	210.27	230.69
Model A	Velocity Angle (β)	^{0}	3.60	4.15	4.58	4.49	4.61
Model B			3.20	3.78	4.26	4.34	4.47

This depicts an increased rise in recirculation with an increase in number of blades up to four blades runner for both model A and model B, at a constant inlet velocity of 20m/s. While deterioration occurs at model A and model B obtaining the same value of vorticity magnitude for 5-blades runner, the 6-blade runner has the highest recirculation value for model A and B.

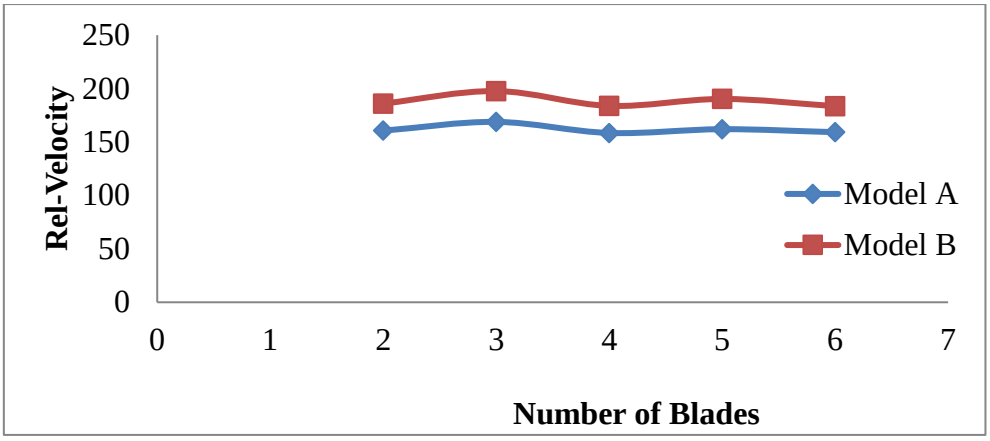

Fig.7.0: Blades number effect on relative velocity magnitude

Fluid Flow Pressure around Different Blades of the Kaplan Turbine

In figure 7.0 shows maximum pressure and minimum pressure value for model A after post simulation analysis had been carried out using ANSYS 16.0. The surface of the blade runners at the suction surface showed higher pressure. However, the runner blade edges and the discharge surface show a negative value of pressure. In figure 4.5, it was observed both 3-blade runner and 5-blade runner has higher operating pressure while the other has minimum operating pressure. 3-blade runner in model A has the highest working pressure above other blades number while two blades runner has the lowest value of pressure followed by 6-blades runner.

Figure 4.6 shows maximum pressure and minimum pressure value for model B after post simulation had been carried out using ANSYS 16.0. The surface of the blade runners at the suction surface with red colour also showed higher pressure. However, the runner blade edges and the discharge surface yellow and blue colour show a negative value of pressure. It was also observed, similar to what obtained in model A, that both the 3-blade and 5-blade runners has higher operating pressure, while the rest with the blue surfaces, were having a minimum operating pressure. 3-blade runner in model B also has the highest working pressure above other blades.

Turbine Blade Power

One of the main considerations in turbine selection for site is in its operational efficiency. The values for turbine blade power, water flow power was generated and computed in Table 8.0. From Figure 8.0, the power output generated by the rotating turbine was at maximum value for Model A at 6-blades. It was observed that the more the runner blade number, the rise in power generated by the blade for model A and model B up to the 6-blade runners. Furthermore, model B can generate more power output than model A at same blade runner.

Table 8.0: Input Power (Water Power), Output Power (Turbine Power) and Efficiency

	Blade Model	Turbine Power (W)	Water Power (W)	Efficiency (%)
2 Blades	A	2146575.982	31180.4964	68.8435474
	B	2500000.98	40522.167	61.69465172
3 Blades	A	3206743.252	43838.928	73.14830445
	B	3637660.681	56731.0338	64.12117737
4 Blades	A	5013673.025	55347.2352	90.58579001

	B	6094975.566	71818.6176	84.86623344
5 Blades	A	5426667.705	65724.8418	82.56646279
	B	7250725.691	86700.78	83.62930173
6 Blades	A	6627350.998	71271.2196	92.98775909
	B	8889699.222	97055.4312	91.59404179

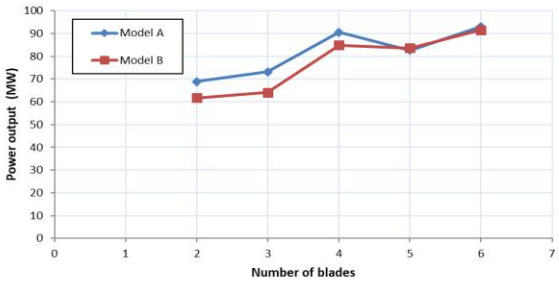

Fig.8.0: Effect of number of blades on Turbine Blade Power

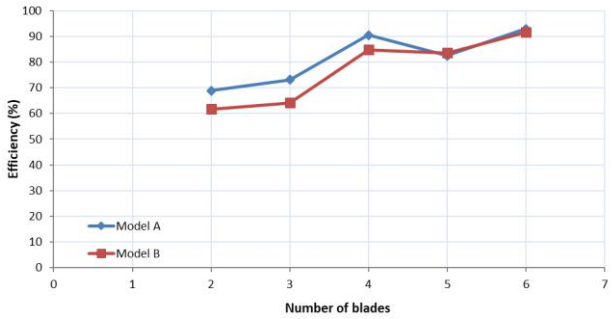

Fig.9.0: Effect of number of blades on efficiency

Turbine Blade Efficiency

The efficiency of a turbine is based on the ratio of turbine blade power and water flow power. The highest efficiency achieved was 92.99% obtained for model-A at 6-blade runners, while 91.59% is known as the highest efficiency for model B at 6-blade runners. The value of efficiency for model A with 6 blades was higher than the 6-bladed runner of model B by 1.4%. The 4-blade runner also gave optimal efficiency of 90.5% and 84.9% for the models A and B respectively. This is similar to the result obtained by Chamil et al. (2017). In his research study on Kaplan turbine design on efficiency, he also observed 4-blade has the highest efficiency.

However, the turbine highest efficiency obtained at 6-blade runners was in support of Chamil *et al.* (2017) result from their theoretical design, though they obtained highest efficiency to be 64.21%. While in their research for efficiency on Kaplan turbine design using Ansys simulation, 4-blade has the highest efficiency. Their record on efficiency was named as an optimized design.

Benchmark of simulation results with performance of similar research work

Figure 10 presents the comparison between result of the simulation and similar research works which also investigated the effect of number of blades on the Kaplan turbine. Chamil and Tobi (2017) designed and investigated the performance of a mini Kaplan hydraulic turbine. He performed a theoretical design where he obtained an efficiency of 59.98%. However, he worked more on adjusting the inlet and outlet angles. He concluded that the runner with 4-blades gave the optimum efficiency. Figure 10 presents the comparison between the efficiency obtained and that which was obtained from the two models. Jawad (2019) also designed and investigated the performance of a Kaplan turbine runner for increased power output and efficiency. From his work, the 3blade runner performed optimally more than the other blade numbers. However, the efficiencies of the two models from the research work gave higher values for the 4-blade runner as well as the 6-blade runner.

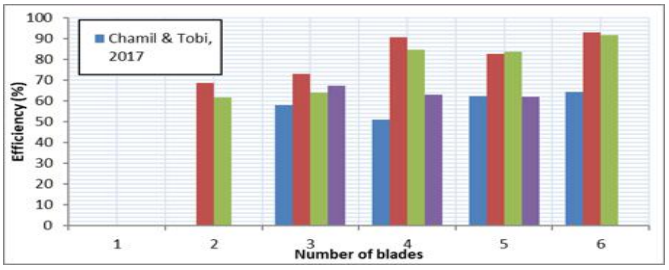

Fig.10: Effect of number of blades on efficiency

I. CONCLUSION

This research study focused on the investigation of the effect of blade number and blade length of the Kaplan hydro-turbine for improved hydrodynamic efficiency. A Kaplan blade turbine was theoretically designed and numerical simulations were carried out in ANSYS Fluent. Two categories of runners with varying number of blades and cross-sectional areas were classified as model A and model B. Based on the results of the CFD, the following conclusions can be made:

1. Model A turbine runner is capable of generating 2.15MW for the 2-blade runner, 3.21MW for the 3-blade runner, 5.01MW for 4-blade runner, 5.43MW for 5-blade runner, 6.63MW for 6-blade runner while model B is capable of generating 2.50MW for 2-blade runner, 3.64MW for 3-blade runner, 6.09MW for 4-blade runner, 7.25MW for 5-blade runner and 8.89MW for the 6-blade runner. The mechanical efficiency for model A is 68.84% for the 2-blade runner, 73.15% for the 3-blade runner, 90.59% for the 4-blade runner, 82.57% for the 5-blade runner and 92.99% for the 6-blade runner. The mechanical efficiency for model B is 61.69% for 2-blade runner, 64.12% for 3-blade runner, 84.87% for 4 blade runner, 83.62% for 5 blade runner and 91.59% for 6 blade runner.
2. The more the addition of blades to the Kaplan runner, the lower the velocity distribution value. The low velocity had an adverse effect on the shaft rotation and hence power output of a turbine. Models A and B's 3-blade runner has the highest flow velocity of 145.29 m/s and 206.94 m/s respectively. 2-blade turbine for model A has the highest-pressure difference with a value of 13.4 MPa while 6-Blade turbine runner for model B is having the highest value of pressure difference with a value of 14.6 MPa. The two models of turbine runner are more prone to cavitation.
3. Also increasing the blade length and in effect the surface area of the Kaplan hydro turbine runner increases the magnitude of the velocity of the runner thus improving the efficiency of the turbine.
4. Simulation results showed that an estimated power 8.89MW was obtained as the optimum power output from the 6-blade runner of model B at efficiency 91.59%.This shows that an increase in blade total surface area, as a result of an increase in blade length or blade number, increases the power output of the Kaplan hydro turbine. However, considering the trade-off of cost of production and operational instability of higher blade runners,4-blade model A runner which gave a power of 5.01MW and an efficiency of 90.58% is recommended for the optimum design of the Kaplan turbine.

REFERENCES

[1] Ajaz. B.J, Shahid. K and S. Muhammad. (2012). Blade Profile Optimization of Kaplan Turbine Using CFD Analysis. *Journal of Eng. & Technology, Mehran University, Pakistan*. Volume 32, No. 4

[2] Balmer, David. (2003). Separation of Boundary Layers, *School of Engineering and Electronics, University of Edinburgh UK.*

[3] Bose.T.K (1997). Numerical Fluid Dynamics. *London: Narosa Publ, House*.

[4] Cengel Y. A. and Cimbala J. M., (2006) Fluid Mechanics; Fundamentals and Applications, New York: Mcgraw-Hill

[5] Chamil. A, Tobi. H., (2017). Design and Analysis of a Kaplan Turbine Runner Wheel. *Proceedings of the 3rd World Congress on Mechanical, Chemical, and Material Engineering (MCM'17). Rome, Italy.*

[6] Chen. J and Engeda. A., (2019). Design considerations for an ultra-low-head Kaplan turbine system. *Earth and Environmental Science*. 240 (2019) 042021

[7] Chica.E, Edwar. A. T, and Arbeláez.J., (2018). Manufacture and experimental evaluation of a hydrokinetic turbine for remote communities in Colombia. *Renewable Energy and Power Quality Journal*, 6(2172-038 X).

[8] Chica.E, P´erez.F, Rubio.A.C & Agudelo.Z., (2016). Design of a hydrokinetic turbine. *Energy and Sustainability*, VI (137).

[9] Diaelhag. Khalifa, (2008). CFD Simulation of Axial Flow Turbine. University of Khartoum.

[10] Dixon.S. L., Fluid Mechanics, and Thermodynamics of Turbomachinery, 5th Edition, Elsevier Butterworth–Heinemann, (2005).

[11] Elbatran, A. H, Abdel-Hamed, M. W, Yaakob O. B., & M. Ahmed, Y., (2015). Hydro Power and Turbine Systems Reviews. *Jurnal Teknologi*, 74(5). 12. https://doi.org/10.11113/jt.v74.4646

[12] Jawad, L. H. (2019). Design and Performance Investigation of a Hydraulic Mini Turbine Based on Renewable Energy Production System. *Journal of University of Babylon for Engineering Sciences.*

[13] Khan M.J., Iqbal M.T. and Quaicoe J.E. (2007). River Current Energy Conversion Systems: Progress, *Prospects and Challenges. Renewable and Sustainable Energy*, 2177-2193.

[14] Nuantong, W. (2009). Flow Simulations on Blades of Hydro Turbine. International Journal of Renewable energy. *Office of Energy Efficiency & Renewable Energy* (OEETE) (2021) Water Power Technologies: Types of Hydropower Turbines; retrieved on the 3rd of August, 2021 from https://www.energy.gov/eere/water/type-hydropower-turbines

[15] Paish, O. (2002). Small hydro power: technology and current status. *Renewable and Sustainable Energy Reviews*, 537- 556.

[16] Plagge A.M, Jestings L, Epps B.P., (2014). Next-generation hydrokinetic power take-off via a novel variable-stroke hydraulic system. *Proceedings of the ASME 2014 33rd international conference on ocean, offshore and Arctic engineering*.

[17] Sotoude.M.H, Haghighi S.M.,MirghavamiS.F., ChiniA.R ., (2019). Developing a method to design and simulation of a very low head axial turbine with adjustable rotor blades. *Renewable Energy*, 266-276.

[18] Styrylski.M, J. Tomalik, and M. M. Grahl, . (2009). Computer Aided Engineering as a Useful Tool in Hydraulic Turbine Design. Krzeszowice in Poland.